Response of the Mössbauer spectrum of paramagnetic Fe^{3+} in Al_2O_3 to nuclear dipole fields

J. Hess and A. Levy*
The Racah Institute of Physics, The Hebrew University of Jerusalem, Jerusalem, Israel
(Received 16 November 1979)

Experimental ^{57}Fe Mössbauer (ME) spectra of $Al_2O_3(Fe^{3+})$ single crystals are presented. Measurements were made down to 60 mK and in applied magnetic fields from 0 to 100 G At 60 mK the ME spectra of the $S_z = \pm\frac{1}{2}$ ionic ground state was isolated, and its response to weak (less than 100 G) applied magnetic fields was examined. A qualitative discussion of the anisotropic response to magnetic fields is given. In zero-applied magnetic field the spectrum is strongly influenced by nuclear dipole fields from surrounding ^{27}Al nuclei. From a theoretical reconstruction of the zero-applied-field spectrum the average magnitude of the ^{27}Al nuclear dipole field is determined to be 4.5 ± 1.5 G. Good agreement is obtained with a theoretical calculation which involves the identical lattice sum which occurs in the Van Vleck formula for the second moment of the nuclear dipole broadening of an NMR line. The connection between the dipole field observed in the ME experiment and the second-moment calculation of the broadening of an NMR line is discussed. Also considered are possible relaxation mechanisms. The spin-lattice relaxation rates are estimated using experimental data for the lattice thermal conductivity and application of the fluctuation-dissipation theorem to the reversible heat flow. It is concluded that at 60 mK relaxation effects are not observed in the ME spectra and also that broadening due to Fe^{3+}-Fe^{3+} interaction is negligible compared to the nuclear dipole broadening, except for a broad single-line contribution in the center of the spectrum.

I. INTRODUCTION

The crystal field (CF) in Al_2O_3 splits the $^6S_{5/2}$ term of Fe^{3+} into three Kramers doublets (CF states) of effective spins $S_z = \pm\frac{1}{2}$, $\pm\frac{3}{2}$, and $\pm\frac{5}{2}$. As verified in previous works,[1,2] the $|\pm\frac{3}{2}\rangle$ CF state is at energy corresponding to temperature 0.5 K above the $|\pm\frac{1}{2}\rangle$ ground state and the $|\pm\frac{5}{2}\rangle$ CF is at 1.5 K above the ground state (Fig. 1).

A Mössbauer (ME) spectrum of ^{57}Fe taken with $H_{\parallel} = 80$ G and at 1.3 K [Fig. 2(a)] shows a superposition of ME spectra corresponding to all three CF states. The two outer lines are the outside lines of the six-line effective-field (EF) spectra corresponding to the $|\pm\frac{5}{2}\rangle$ CF state. The next two lines in from the outside line are the outside lines corresponding to the $|\pm\frac{3}{2}\rangle$ CF state. The splittings of the corresponding pairs are in the proper ratio (5:3) expected for effective-field ME spectra. In Fig. 2(b) taken at 0.6 K the $|\pm\frac{5}{2}\rangle$ CF state is almost completely depopulated and one observes a superposition of the $|\pm\frac{3}{2}\rangle$ ME spectrum and the $|\pm\frac{1}{2}\rangle$ ME spectrum. At 60 mK [Fig. 2(c)] the $|\pm\frac{3}{2}\rangle$ CF state is also depopulated and the ME spectrum corresponding to the $|\pm\frac{1}{2}\rangle$ CF ground state is obtained.

The ME spectrum of Fig. 2(c) is not an EF spectrum. Experimentally this refers to two properties. One is that the ME spectrum does not have the standard six-line (or four-line if only circularly polarized γ's are observed) form of an ^{57}Fe ME spectra in magnetic iron, where total splitting is proportional to the effective electron spin of the ionic state. The other is that the ME spectrum is extremely sensitive to the magnitude and direction of applied magnetic field. Compare the experimental spectra of Fig. 2(c), with that of Fig. 5 which differs in the direction of the applied magnetic field.

Sensitivity to weak applied magnetic field is a property of the $|\pm\frac{1}{2}\rangle$ CF ground state only. The excited CF states have EF spectra and show no response to applied fields up to 2 kG, where mixing between the CF states occurs.[1]

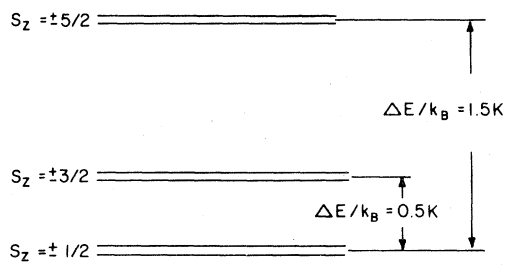

FIG. 1. Energy-level scheme of the crystal-field levels of dilute Fe^{3+} in the Al_2O_3 lattice.

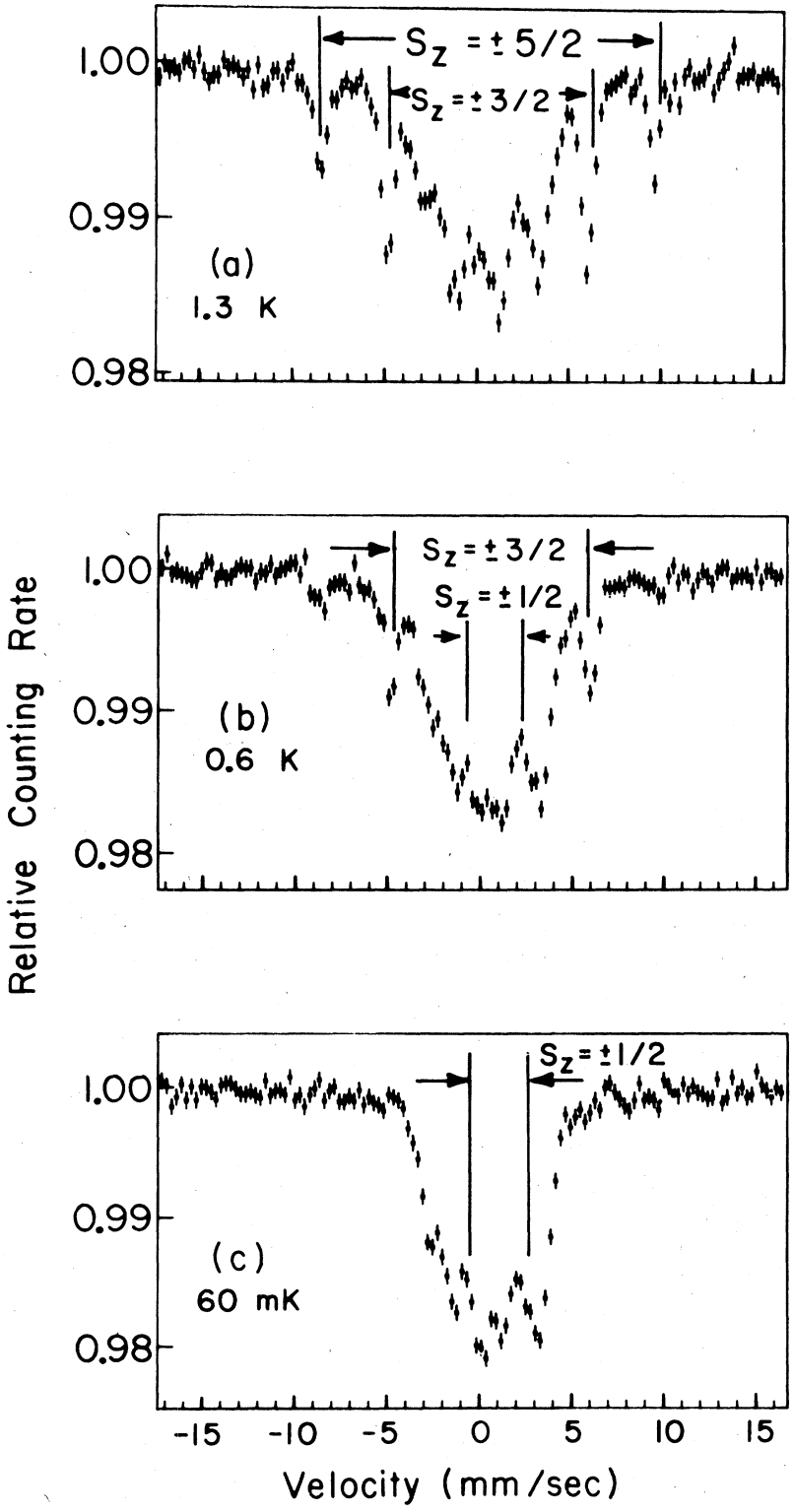

FIG. 2. ^{57}Fe Mössbauer spectra at various temperatures with $H_{\parallel} = 80$ G. Spectra show the superposition of contributions from the three crystal-field levels. Effective-field splittings corresponding to each CF state are indicated. Note that the $S_z = \pm \frac{1}{2}$ contribution is broader than the corresponding effective-field splitting.

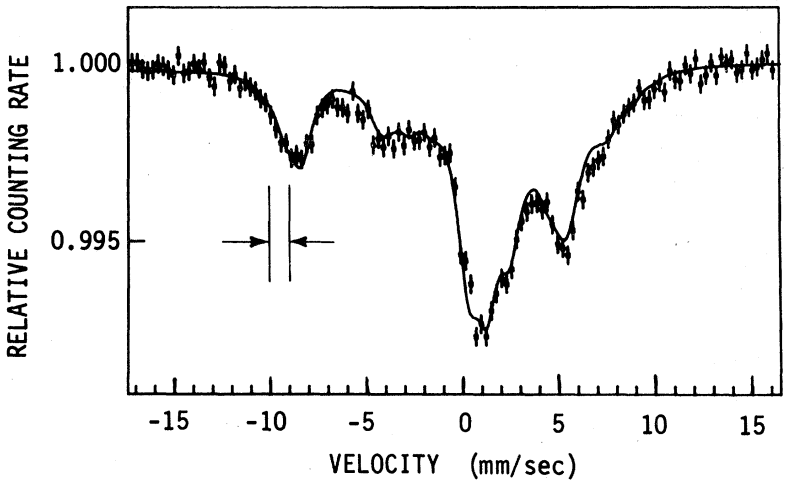

FIG. 3. ^{57}Fe Mössbauer spectrum taken at 60 mK with no applied external field. The spectrum shows nuclear dipole broadening. The theoretical fit to the experimental points is discussed in Sec. IV. Interval indicated between the arrows is the instrumental linewidth.

This paper deals with the weak field (less than 100 G) non-EF response of the $|\pm\frac{1}{2}\rangle$ CF ground state. The main experimental result is the observation of broadening of ^{57}Fe ME lines in Al_2O_3 due to nuclear dipole interactions with ^{27}Al nuclei adjacent to the ME nuclei. Such a broadened spectrum is shown in Fig. 3 which may be compared with a nonobservable theoretical spectrum for zero field in Fig. 4(a). In Sec. IV it is determined from the ME spectrum of Fig. 3 that the average magnitude of the nuclear dipole field from ^{27}Al spins at Fe^{3+} ions is 4.5 ± 1.5 G.

II. DESCRIPTION OF EXPERIMENT

Measurements were carried out on $Al_2O_3(Fe^{3+})$ single crystals kindly provided to us by Dr. G. K. Wertheim. The crystals were identical to those used in previous ME work[1,3] on $Al_2O_3(Fe^{3+})$ and have an Fe^{3+} concentration of 0.08 at.%. The Fe^{3+} was isotopically enriched to over 90 at.% ^{57}Fe. The crystals were placed inside the mixing chamber of a dilution refrigerator[4] with the c axis oriented along the propagation direction of the γ rays. Clear Mylar windows for the incident γ rays were used throughout the system. Some thin layers of iron-free aluminum foil were used in the dilution refrigerator for radiation shielding. Resonant ^{57}Fe ME background in the absence of the Al_2O_3 crystals was about 0.015%.

To obtain ME spectra, a high-speed counting system was used, including a proportional counter with Mylar window and an intense (~ 50 mCi) ^{57}Co Mössbauer source (^{57}Co in Rh). With this system it was possible to obtain a counting rate of about 50 000 sec^{-1} on the 14.4-keV Mössbauer line of which about 2% was resonantly absorbed by the ^{57}Fe in the Al_2O_3. External magnetic fields were applied either parallel or perpendicularly to the c axis of the Al_2O_3 crystals with a pair of Helmholtz coils. The homogeniety of the applied field in the region of the crystals was better than 1%.

ME spectra were recorded for a velocity range of ± 15 mm/sec and the instrumental linewidth was 0.9 mm/sec.

For all the measurements the ionic spins, constrained along the c axis by the CF field, determined a macroscopic axis of quantization, independent of the relatively weak external fields which were applied. Only circularly polarized components of the ME spectrum corresponding to nuclear transitions such that $\Delta m_I = \pm 1$ were observed.

III. STATIC RESPONSE OF THE $|\pm\frac{1}{2}\rangle$ CF GROUND STATE ME SPECTRUM TO WEAK MAGNETIC FIELDS (LESS THAN 100 G)

As indicated in the Introduction the response of the ground-state ME spectra to weak magnetic fields is complex and is characterized by sensitivity to the magnitude and direction of the applied field. This is in contrast to the responses of the excited CF states whose ME spectra are insensitive to small external fields, whatever their direction.

A sampling of the variety of ME spectra which may be considered for the CF ground state is shown in Fig. 4. Relevant to the analysis of the experimental spectrum of Fig. 3 are the spectra of Figs. 4(c) and 4(d). For $H_\parallel = 5$ G [Fig. 4(c)] the ME spectrum is almost identical to the ideal zero-field spectrum of Fig. 4(a), whereas for $H_\perp = 6$ G [Fig. 4(d)] the zero-field spectrum is almost unrecognizable. If it were

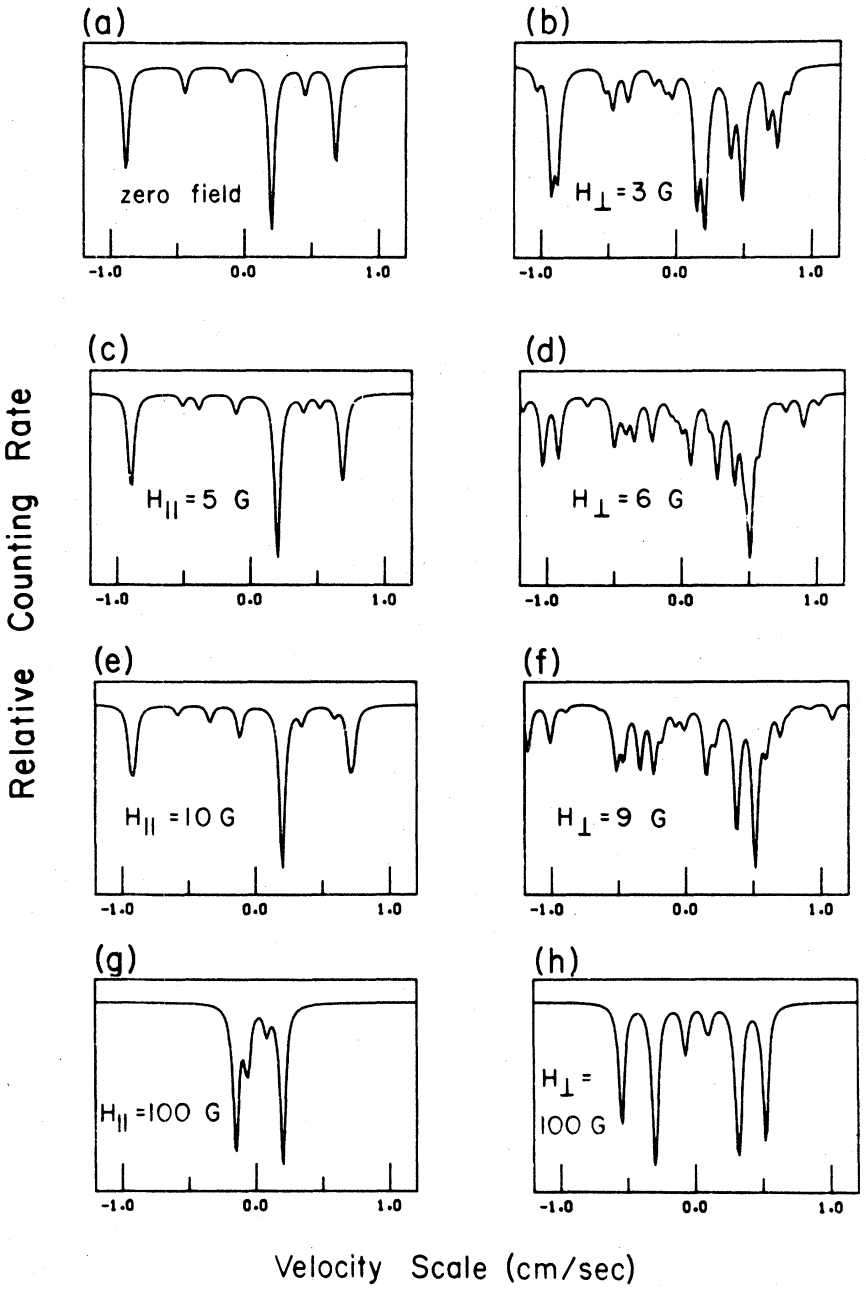

FIG. 4. (a)–(h) Theoretical magnetic-field responses of the Mössbauer spectra of the CF ground state calculated from the full Hamiltonian [Eq. (1)]. Note that the spectra are more sensitive to fields $H_\perp$ applied perpendicular to the c axis than to fields $H_{||}$, parallel to the c axis.

possible to devise a method of orienting the ^{27}Al spins along the c axis, in zero applied field, then the spectrum of Fig. 4(a) might actually be observable. For larger applied fields the theoretical spectra are almost realized experimentally [compare Fig. 4(h) with Fig. 5 for $H_\perp = 27$ G]. For $H_\perp = 27$ G broadening from uncorrelated ^{27}Al spins is less pronounced than for smaller fields and a spectrum identical to the EF spectrum of the $|\pm\frac{3}{2}\rangle$ CF state is approached. The outer lines of the limiting $|\pm\frac{3}{2}\rangle$ EF spectrum may be seen in Figs. 2(a) and 2(b). The approach to this limiting EF spectrum is discussed in an article by Afanas'ev and Kagan.[5]

The coupled electronuclear states between which

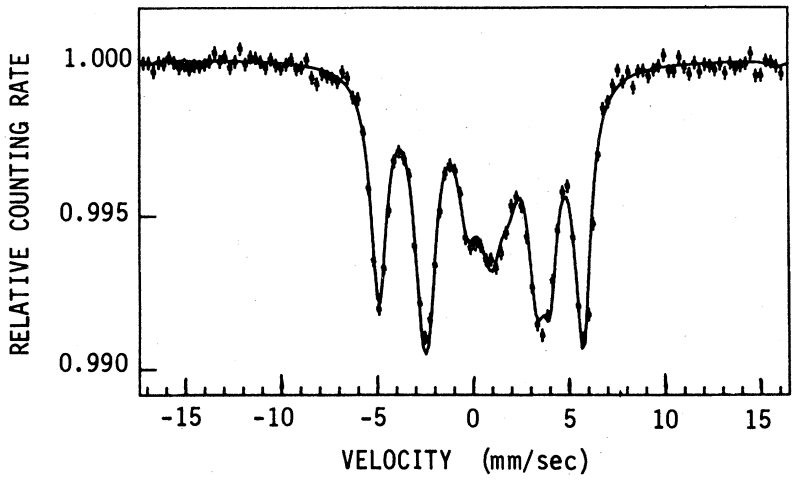

FIG. 5. ^{57}Fe Mössbauer spectrum taken at 60 mK with applied field $H_\perp = 27$ G. Total splitting is the same as that of an $S_z = \pm\frac{3}{2}$ effective-field spectrum albeit the CF state is the $S_z = \pm\frac{1}{2}$ ground state. The theoretical fit is discussed in Sec. IV.

ME transitions occur are given by the Hamiltonian

$$\mathcal{H} = H_\parallel g_\parallel \mu_B S_z + H_\perp g_\perp \mu_B \tfrac{1}{2}(S_+ + S_-) + A_\parallel I_z S_z + \tfrac{1}{2}A_\perp(S_+ I_- + S_- I_+) \ , \quad (1)$$

where parallel and perpendicular refer to the crystalline c axis, μ_B is the Bohr magneton, and $H_\parallel$ or $H_\perp$ are the applied magnetic field components. The electronic g factors $g_\parallel$ and $g_\perp$ and the space $|Sm_s\rangle$ in which the electronic spin operators $\vec{S}$ operate are the same for ground and excited ME states. The hyperfine constants $A_\parallel$ and $A_\perp$ and the spaces in which the nuclear spin operators $\vec{I}$ operate differ for the ground and excited ME states. This is so since the ME transition operator is nuclear and acts between $|I = \frac{3}{2}\rangle$ and $|I = \frac{1}{2}\rangle$ states. In ME velocity units[1] $A^e = 1.49$ mm/sec and $A^g = -2.61$ mm/sec. For both excited and ground nuclear states $A_\perp = 3A_\parallel$. The approach of the experimental spectrum Fig. 5 to the EF spectrum of the $|\pm\frac{3}{2}\rangle$ CF state, when in fact the $|\pm\frac{1}{2}\rangle$ CF state is being observed, gives experimental verification to this assumed ratio. It also follows for the "weak" CF case considered here and for negligible nuclear Zeeman interaction that $A_\perp = 3A_\parallel$ implies $g_\perp = 3g_\parallel$ (see Abragam and Bleaney[6]).

Whereas the nuclear transition connects only nuclear states $|Im_I\rangle$, the applied magnetic field operates only in the electron spin space $|S = \frac{1}{2}\ m_s\rangle$. The uncoupled states $|m_s\rangle\ |m_I\rangle = |m_s m_I\rangle$ are then natural for describing the ME spectra in weak fields.

The theoretical spectra of Fig. 4 are calculated by diagonalizing the Hamiltonian (1) in the $|m_s m_I\rangle$ representation for the $I = \frac{1}{2}$ nuclear ground state and the $I = \frac{3}{2}$, 14.4-keV nuclear ME state. This gives two sets of electronuclear states between which the ME transitions occur. If ϕ_e is an excited electronuclear (EN) state and ϕ_g is a ground EN state then intensities of the ME lines are proportional to the squared matrix elements $|\langle\phi_e|M_1(I,I')|\phi_g\rangle|^2$ where $M_1(I,I')$ is a dipole operator which connects nuclear states of spins I and I'. Further details of the full calculation are given in the work of Levy.[7]

We wish to give a qualitative discussion of the ME spectra which retains the feature of the anisotropic response in weak fields. For this purpose it is sufficient to consider a spherically symmetric hyperfine (hf) interaction $A\,\vec{I}\cdot\vec{S}$, where $A = A_\parallel = A_\perp$. In this case the coupled EN states are given by

$$|FM_F\rangle = \sum_{M_I M_s} (ISFM_F|IM_I SM_s)|M_s M_I\rangle$$

where $\vec{F} = \vec{I} + \vec{S}$ and $(ISFM_F|IM_I SM_s)$ are vector-coupling coefficients. For the excited $I = \frac{3}{2}$ nuclear state the EN states have angular momentum $F = 1, 2$ and for the ground nuclear state $F = 0, 1$. The $M1$ transition operator acts only between nuclear states so for a ME transition where $\Delta M_s = 0$, M_F has the same selection rules as M_I, i.e., $\Delta M_F = 0, \pm 1$. Of these only the $\Delta M_F = \pm 1$ components are observable. The $|FM_F\rangle$ level scheme with ME transitions is shown in Fig. 6. ME transition intensities indicated in Fig. 6 are proportional to the squared matrix elements $|\langle FM_F|M_1(I,I')|F'M_{F'}\rangle|^2$. The actual ME spectrum of Fig. 3 requires consideration of an additional term in the hf interaction,

$$(A_\perp - A_\parallel)(S_+ I_- + S_- I_+) \ .$$

However, even with neglect of this term, the three main lines which characterize the spectrum of Fig. 6 still persist as a feature of the actual spectrum of Fig. 3.

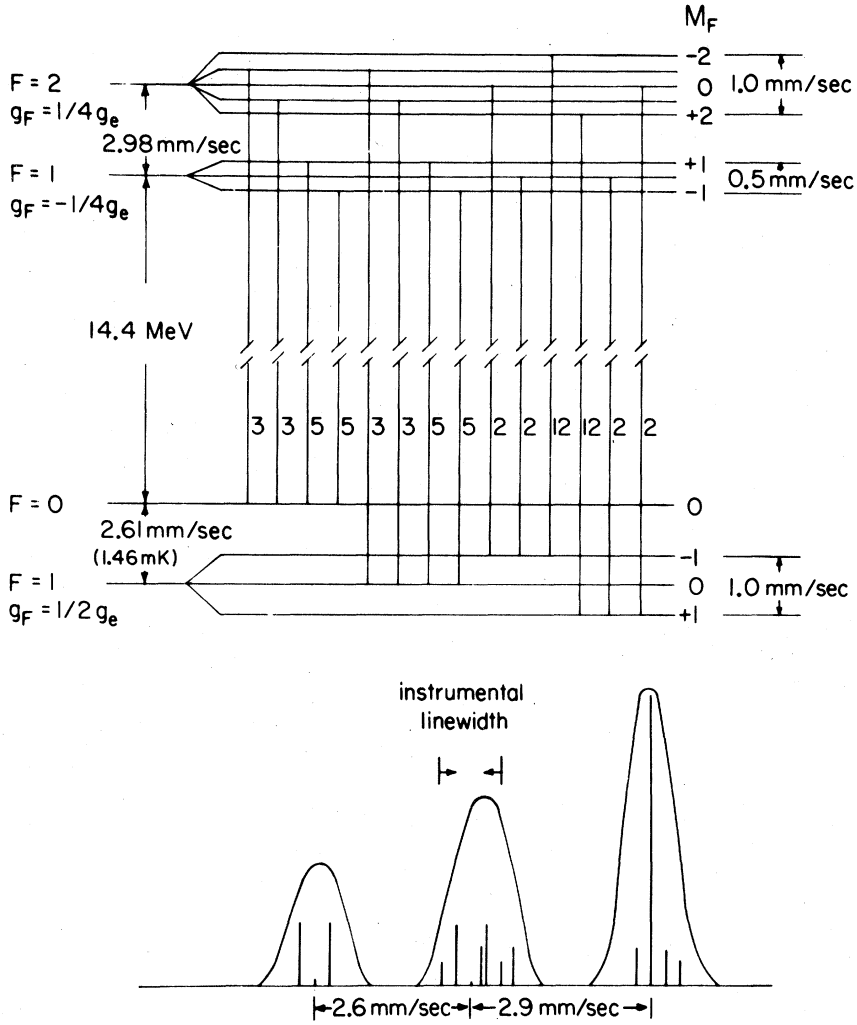

FIG. 6. Level scheme of coupled electronuclear states and $M_F = \pm 1$ Mössbauer transitions for a spherically symmetric hyperfine interaction. The three-line spectrum is shown broadened by a 4.5-G field applied parallel to the quantization axis. For the actual specrtrum (Fig. 3), where $A_\perp = 3A_\parallel$, the overall splittings are larger but the three lines seen here are still observable. Numbers marking the various transition lines are relative intensities. Also indicated on the ME spectrum is the instrumental linewidth.

For a spherically symmetric A and g tensor[6] the anisotropic weak-field response is caused only by the asymmetry introduced by the macroscopic quantization axis of the single crystals. Electron spins and, via the hf interaction, F spins are constrained by the CF interaction to lie along the crystalline c axis. For external field $H_\parallel$ applied parallel to the c axis the $|FM_F\rangle$ representation completely describes the response of the ME spectrum. There is no breaking of the F-rank rotational symmetry. The rotational symmetry, though, refers only to the c axis. The Landé splitting factors g_F which reflect this symmetry and describe the parallel response do not describe the perpendicular response. This is the origin of the different responses for $H_\parallel$ and $H_\perp$.

For free atoms, Landé splitting factors describe the magnetic response for all directions of applied field since a free atom may align itself in the field. In our case the "free-atom" response is obtained for $H_\parallel$ only and it is the field which is aligned along the atomic moments, rather than vice versa.

The response for $H_\parallel = 4.5$ G (magnitude of the nuclear dipole field) is detailed in Fig. 6. The g_F are approximately equal to $(S/F)\cos(\vec{S},\vec{F})g_e$ (where $g_e = 2$, the free-electron g factor) and take values of 1 or $\frac{1}{2}$ (Fig. 6). For 4.5 G the result is broadening the order of 0.6 mm/sec, the order of a linewidth.

For $H_\perp = 4.5$ G, the response is very different. Since the Fe^{3+} ions are not free to turn in the perpendicularly applied field, the rotational symmetry

represented by the $|FM_F\rangle$ states is broken (the states which describe the response are mixtures of $|FM_F\rangle$ states). The g factors, which reflect the symmetry of the representation which describes the perpendicular response, are 2 or larger. They are then larger than the g_F, which reflect F-rank rotational symmetry about the c axis, by a factor of 2 or 4.

The above illustration for a spherically symmetric A and g tensor draws attention to the role of the macroscopic symmetry axis in describing the response of the ME spectra. In the actual case $g_\perp = 3g_\parallel$, which introduces an even larger difference between parallel and perpendicular responses.

If matrix elements involving $A_\perp$ vanish, as for the excited CF states, then symmetries of the $|SM_s\rangle$ space are not correlated to symmetries in the nuclear $|IM_I\rangle$ spaces. Hence the applied field has no effect upon the ME spectra. This is the effective-field case.

IV. THEORETICAL FITTING OF THE ME SPECTRUM FOR ZERO-APPLIED FIELD

In constructing the theoretical ME spectra used to fit the experimental spectrum of Fig. 3, the broadening due to Fe^{3+}-Fe^{3+} interactions is neglected and only the magnetic-field contributions of ^{27}Al nuclei are considered. To justify this we first calculate the average magnitude from neighboring Fe^{3+} ions compared with the average magnitude from ^{27}Al nuclear spins. The average atomic concentration of Fe^{3+} ions compared to Al atoms[8] or nuclei is 0.0008. The magnitude of a dipole field varies as $1/r^3$ where r is the distance from the source. Since

$$\left\langle \frac{1}{r^3} \right\rangle_{Fe^{3+}-Fe^{3+}} = 0.0008 \left\langle \frac{1}{r^3} \right\rangle_{Fe^{3+}-Al^{3+}} ,$$

the average ratio of the respective field contributions from Fe^{3+} and ^{27}Al is

$$\frac{(1837)(2)\frac{1}{2}0.0008\mu_N}{3.641\mu_N} = 0.4 ,$$

where $(1837)(2)\mu_N$ is the effective moment of the Fe^{3+} state (only the $|S=\frac{1}{2}\rangle$ CF state contributes), $3.641\mu_N$ is the magnetic moment[9] of ^{27}Al, and μ_N is a nuclear magneton.

Anticipating the result of 4.5 ± 1.5 G for the average nuclear dipole-field magnitude then gives an average value of 1.8 G for the Fe^{3+} contribution at the average Fe^{3+}-Fe^{3+} separation.

There are also constraints which reduce the effect of the Fe^{3+} fields. The CF interaction constrains electronic spins along the c axis. The components of the dipolar field from an electronic spin at distance r from the ME nucleus are

$$H_\parallel = (\mu/r^3)2P_2(\cos\theta) ,$$

$$H_\perp = (3\mu/r^3)\sin\theta\cos\theta ,$$

where θ is the angle between the vector connecting the Fe^{3+} source point to the ME nucleus and the c axis. $H_\perp$ contributions are then zero for collinear sites ($\theta = 0°$) or for $\theta = 90°$. In a detailed statistical model $H_\perp$ from noncollinear sites is compensated almost completely and does not introduce changes. For averagely spaced (about 11 lattice sites apart) uncompensated Fe^{3+} ions, the $H_\parallel$ contribution is about 1.8 G. Due to the insensitivity to parallel fields this contribution causes negligible change in the ME spectrum. On the other hand, an uncompensated collinear Fe^{3+} spin in adjacent or next-neighbor site (a nonaverage situation) can contribute a parallel field of hundreds of gauss, sufficient to collapse the ME spectrum into a single broad line. If we partition the contributions into those for $H_\parallel$ larger than 100 G which collapse the spectrum entirely and those for $H_\parallel$ less than 30 G , which hardly affect the ME spectrum [Figs. 4(a), 4(c), and 4(e)], then in a detailed statistical model in three dimensions there remain less than 1% of the Fe^{3+} ions occupying sites which contribute a $H_\parallel$ of 30–100 G. A 30–100-G field seriously distorts the spectrum; however, since the contribution of these Fe^{3+} ions is less than 1% their effect is neglected.

The contributions of first, second, and third collinear nearest-neighbor sites are taken into account by a Gaussian-shaped contribution to the ME spectrum centered around $V = 0$ of about 3.5-mm/sec width. This contribution also includes the contributions of nonsubstitutional Fe^{3+} ions and also nonstatistical clustering of Fe^{3+} ions. It has been observed that this contribution is always about $7 \pm 2\%$ and temperature independent.[7] It also includes an instrumental contribution from the thin windows.

Construction of the theoretical ME spectrum of Fig. 3 was then carried out as follows. The applied field is assumed to consist of a contribution h_n from ^{27}Al moments of random direction and a directed component h^0 (about 1.0 G) from the laboratory which was not shielded out. The ME spectra were then numerically averaged over 4π solid angle as follows. ϕ_l and θ_m are azimutal and polar angles giving the direction of the h_n field with respect to the c axis and some axis perpendicular to the c axis. l and m refer to a finite cell $\Delta\Omega_{lm}$ in the solid-angle phase space in which the averaging was carried out, where $\Delta\Omega_{lm} = \sin\theta_m \Delta\phi_l \Delta\theta_m$. The actual field considered then has components

$$h_x(n,m,l) = h_x^0 + h_n \sin\theta_m \sin\phi_l ,$$

$$h_y(n,m,l) = h_y^0 + h_n \sin\theta_m \cos\phi_l ,$$

$$h_z(n,m,l) = h_z^0 + h_n \cos\theta_m .$$

For each h_n and lm cell in the angular phase space a ME spectrum $S_{n,l,m}(v)$ was calculated from the electronuclear states of the full Hamiltonian (1). The

Hamiltonian is independent of the azimutal angle ϕ_1. ϕ_1 dependence is introduced from the directed field contribution of the laboratory. The h_n are assumed to follow a Gaussian distribution centered around zero (the macroscopic average of the ^{27}Al dipole field is zero) and of average field width $2\Delta h$. The resultant ME spectrum is then a superposition of $S_{n,l,m}(v)$ spectra given to within a normalization factor by

$$S(v)=\sum_{nlm}\exp[-(h_n/2\Delta h)^2]\sin\theta_m S_{nlm}(v) \ .$$

The collapsed component of the experimental spectrum was obtained from a number of different experimental spectra[7] at different temperatures. The free parameters used to fit the experimental "zero-field" spectrum were the vector $\vec{h}^0$ of the laboratory field and the average magnitude Δh of h_n of the ^{27}Al dipolar fields. Optimum values from a least-squares computer fit were

$$\begin{aligned}&\Delta h=4.5\pm1.5 \text{ G} \ ,\\ &|\vec{h}^0|=1.2\pm0.6 \text{ G} \ .\end{aligned} \tag{2}$$

Δh may be estimated from a lattice sum over the ^{27}Al contributions whose directions are uncorrelated. Suppose the z direction (here not necessarily the c axis) is the direction of the nonzero resultant. Contributions to the resultant are then (μ^2/r_i^3) $(1-3\cos^2\theta_i)$ for each neighboring moment μ and the mean square average $\langle\Delta h^2\rangle$ is given by the lattice sum

$$\langle\Delta h^2\rangle=\mu^2\sum_i\frac{1}{r_i^6}(1-3\cos^2\theta_i)^2 \ .$$

θ_i is the angle between the resultant direction and the contributing ^{27}Al spin. Averaging over the uncorrelated spin directions θ_i gives

$$\langle\Delta h^2\rangle=\tfrac{4}{5}\mu^2\sum_i\frac{1}{r_i^6} \ . \tag{3}$$

This formula may be compared to the Van Vleck formula[10] for the second moment $M_2=\langle\Delta\omega^2\rangle$ of an NMR line broadened by nuclear dipole-dipole interactions, where the polycrystalline average is taken. Taking the correspondence $M_2=\langle\Delta\omega^2\rangle=\gamma^2\langle\Delta h^2\rangle$ where $\gamma^2=\mu^2/[\hbar^2 I(I+1)]$, Eq. (3) is seen to differ from the Van Vleck formula by a factor $\frac{4}{3}=(3)\frac{4}{9}$. The $\frac{4}{9}$ factor comes from neglecting the adiabtic flip-flop term[10] in the nuclear spin-spin interaction and the factor 3 arises from the fact that the resultant $\langle\Delta h^2\rangle$ must in the NMR case still be projected along the direction of the external field, whereas in the ME case the full magnitude $\langle\Delta h^2\rangle$ is observed. $\Delta\vec{h}$, as we have introduced it, is an isotropic vector whose directions in the $\Delta\Omega_{lm}$ phase space are all equiprobable. Thus $\langle\Delta h_x^2\rangle=\langle\Delta h_z^2\rangle=\langle\Delta h_y^2\rangle=\frac{1}{3}\langle\Delta h^2\rangle$. A more correct correspondence then is $\langle\Delta\omega^2\rangle_{\text{NMR}}=\frac{1}{3}\gamma^2\langle\Delta h^2\rangle_{\text{ME}}$; i.e., $\langle\Delta h_z^2\rangle=\frac{1}{3}\langle\Delta h^2\rangle_{\text{ME}}$.

A lattice sum over neighboring ^{27}Al sites in Al_2O_3 using Eq. (3) gives $\Delta h=3.4$ G.[7] If the quantum-mechanical flip-flop interaction is considered in addition to the static interaction, then Δh (theoretical) is multiplied by a factor $\frac{3}{2}=\sqrt{9/4}$, giving $\Delta h=5.1$ G. This value is in better agreement with the experimental value $\Delta h=4.5\pm1.5$ G.

To justify the assumption of uncorrelated spin directions of ^{27}Al spins, the nuclear-spin system is considered to be in thermal equilibrium with the lattice at 60 mK. The nuclear spin-spin interaction energy corresponds to a temperature of 0.4 μK and so the ^{27}Al nuclear spin states may be considered to be equally and randomly populated.

A similar theoretical fitting procedure has been carried out on the experimental spectrum of Fig. 5 for applied $H_\perp=27$ G. Here the nuclear dipole-dipole broadening has less effect.

V. HEAT FLOW AND RELAXATION PROCESSES WHICH MAY EFFECT THE ME SPECTRA OF THE CF GROUND STATE

In this section it is shown that relaxation effects upon the ME spectra may be neglected.

Consider a closed system consisting of lattice phonons and localized quantum systems described by electronuclear states of the Hamiltonian [Eq. (1)] of ^{27}Al nuclear spin states in an average dipole field of 4.5 G. The combined system of lattice plus localized quantum systems is insulated adiabatically at an equilibrium temperature T. The energy exchange between the macroscopic lattice with continuous energy spectra and the microscopic quantum systems with discrete spectra is described by the microscopic fluctuation dissipation (FD) theorem.[11] The response of the continuous system to a discrete energy input or output $\hbar\omega$ is a fluctuation in its energy with a spectral component of the frequency ω. There is thus an energy flow in both directions between the lattice system and the localized systems which establishes and maintains thermal equilibrium. A part of such processes are transitions between discrete states, or relaxation, of the quantum systems.

In equilibrium, the combined system maintains constant entropy. If $\vec{Q}$ is a local heat-flux vector and T the equilibrium temperature, then

$$\text{div}\left(\frac{\vec{Q}}{T}\right)=\frac{1}{T}\text{div}\vec{Q}-\frac{\vec{Q}}{T^2}\text{grad}T=0 \ ,$$

since the equilibrium value of T is a fixed constant the divergence of the internal heat flux is

$$\text{div}\vec{Q}=\frac{1}{T}\vec{Q}\,\text{grad}T \ .$$

The heat flow is also described by the Fourier law

$$\vec{Q} = -\kappa \,\mathrm{grad} T \ ,$$

where κ is the bulk thermal conductivity. A thermal gradient results in an energy input into a microscopic volume $\Delta V = l^3$ given by

$$\frac{dE}{dt} = (\mathrm{div} Q)\, l^3 = -\kappa (\mathrm{grad} T)\, l^2 \left(\frac{\mathrm{grad} T}{T} \right) l \ .$$

Application of the FD theorem requires a decomposition of dE/dt into spectral components of a "driving force" f_ω and a velocity or flux ωX_ω which is caused by the force.[12] For the driving force we take the fractional temperature difference from equilibrium temperature T across ΔV,

$$f_\omega = \left(\frac{\mathrm{grad} T}{T} \right)_\omega l$$

and for the displacement velocity we take the corresponding heat flow

$$\omega \vec{X}_\omega = \vec{Q}_\omega l^2 = -\kappa (\mathrm{grad} T)_\omega l^2 \ .$$

The impedance, which for heat flow is purely dissipative, is

$$a'' = X_\omega / f_\omega = \kappa (\mathrm{grad} T)_\omega l^2 \frac{1}{\omega} \frac{T}{(\mathrm{grad} T)_\omega} \frac{1}{l} = \frac{\kappa l T}{\omega} \ .$$

Application of the FD theorem then gives the fluctuating temperature squared which is required to maintain equilibrium.

$$\langle f^2 \rangle_\omega = \frac{\langle \Delta T^2 \rangle_\omega}{T^2} = \frac{\hbar}{2\pi} \frac{\omega}{\kappa T l} \coth \left(\frac{\hbar \omega}{2 k_B T} \right) \ .$$

For a lattice temperature $T = 60$ mK, the discrete energies $\Delta E = \hbar\omega$ of the localized systems are much smaller than $k_B T$ ($\Delta E \simeq 3$ mK for the coupled electronuclear system and 0.25 μK for the ^{27}Al spin systems). For $\Delta E \ll k_B T$ the temperature fluctuation takes the form

$$\frac{\langle \Delta T^2 \rangle_\omega}{T^2} = \frac{k_B}{\pi l \kappa} \tag{4}$$

which is the "high-temperature" or "white-noise" approximation. The energy squared associated with the temperature fluctuation squared $\langle \Delta T \rangle_\omega$ is

$$\langle E^2 \rangle_\omega = C_v^2 \langle \Delta T^2 \rangle_\omega \ ,$$

where C_v is the specific heat of a localized system. $\langle E^2 \rangle_\omega$ is the energy available at the transition frequency ω in a volume $\Delta V = l^3$ which contains one localized system. The transition or relaxation rate between discrete states of the localized system is then

$$\frac{1}{T_1} = \frac{2\pi}{\hbar^2} \langle E^2 \rangle_\omega = \frac{2\pi}{\hbar^2} C_v^2 \langle \Delta T^2 \rangle_\omega \ .$$

Substituting Eq. (4) for $\langle \Delta T^2 \rangle_\omega$ gives

$$\frac{1}{T_1} = \frac{2}{\hbar^2} \frac{k_B}{l \kappa} C_v^2 T^2 \ . \tag{5}$$

T is the equilibrium temperature (60 mK). l is the linear dimension of the volume associated with a single localized system, and C_v is the specific heat of this system. κ is the thermal conductivity of the $Al_2O_3(Fe^{3+})$.

The actual transition rate is the product of the above $1/T_1$ times a squared matrix element of the interaction which describes the coupling of the localized system to the lattice. The interactions used are Kronig-Van Vleck or nuclear quadrupole coupling and reduce the transition rate by a factor of about 10^{-4} to 10^{-6}.

The main justification for the above procedure is the availability of accurate experimental values for the lattice thermal conductivity κ so that the lattice contribution to the relaxation times may be estimated without reference to a theoretical phonon spectrum. At 60 mK, for corrundum crystals with dimensions the order of 1 mm, the thermal conductivity is conditioned by boundary scattering of phonons.[13] The phonon mean free path is determined by the crystal dimensions and κ is proportional to T^3. Interpolation of experimental data[14] for synthetic sapphire crystals gives

$$\kappa = 6.20 \times 10^4 T^3 \frac{\mathrm{erg}}{\mathrm{sec\,cm\,K}} \ . \tag{6}$$

The specific heat C_v may be calculated from the energy spectra. For systems with discrete finite energy spectra E_i such that $E_i \ll k_B T$, as is the case here, the specific heat of a single system is

$$C_v \simeq \frac{1}{k_B T^2} \sum_{i=1}^{N} E_i^2 \ ,$$

where N is the number of states. In terms of equivalent temperatures $k_B T_i = E_i$,

$$C_v = \frac{k_B}{T^2} \sum_{i=1}^{N} T_i^2 \ . \tag{7}$$

Substituting Eqs. (6) and (7) into Eq. (5) gives for the relaxation time (in sec^{-1})

$$\frac{1}{T_1} = \frac{75.6}{lT} \left[\frac{\sum T_i^2}{T^2} \right]^2 \mathrm{sec}^{-1} \ , \tag{8}$$

where l is the linear dimension in cm of the volume occupied by the localized system with energy spectra $E_i = k_B T_i$. For a lattice temperature of 60 mK, we consider two cases. One is the electronuclear states of Fe^{3+} where the average lattice spacing is about 400 Å and the other is an $I = \frac{5}{2}$ ^{27}Al spin system with $l \simeq 40$ Å. For the EN states of Fe^{3+}, the average energy corresponds to a temperature $T_i \simeq 3$ mK and

$N = 8$ for the $I = \frac{1}{2}$ ^{57}Fe ground state. This gives, using the average level spacing,

$$\sum_{i=1}^{N} T_i^2 = 7.2 \times 10^{-5}\ \mathrm{K}^2$$

with $l = 4 \times 10^{-6}$ cm. For an ^{27}Al spin system

$$\sum_{i=1}^{N} T_i^2 = (0.25\ \mu\mathrm{K})^2 \sum_{m=-5/2}^{5/2} m^2 = \frac{1}{16}\frac{35}{4} \times 10^{-12}\ \mathrm{K}^2$$

$$= 5 \times 10^{-13}\ \mathrm{K}^2$$

with $l = 4 \times 10^{-7}$ cm. Substituting into Eq. (8) gives relaxation rate $1/T_1 = 1.26 \times 10^5$ sec^{-1} or $T_1 = 8$ μsec for the EN states. The corresponding time for an ^{27}Al spin is the order of 10^{10} sec and outside the range of the experiment. As mentioned, the spin-lattice coupling is very weak and can lengthen the relaxation times by a factor of 10^4 to 10^6. Thus T_1 (Fe^{3+}) may become the order of a second.

Although they are disconnected from the lattice, the ^{27}Al spins may be considered to relax rapidly between themselves via the ^{27}Al-^{27}Al dipole interaction. The relaxation time for this process is the order of the inverse Lamour frequency corresponding to 0.25 μK (the energy of the interaction) and thus is about 0.20 msec. Thus the ^{27}Al spins reach a spin temperature T_s rapidly, which justifies the previous assumption of Sec. IV that ^{27}Al spin directions are uncorrolated over a time of the measurement (~ 18 h). If or how T_s reaches the lattice temperature $T = 60$ mK is unclear. Presumably a coupling of the Fe^{3+} systems to the ^{27}Al spin speeds up the process. T_s goes unobserved in the ME experiment.

The picture used to describe the relaxation of the electronuclear states breaks down as T approaches 0.5 K, the temperature corresponding to the first excited CF state. At such temperatures the assumption $E_i << k_B T$ breaks down and a different relaxation regime is approached. Likewise for $T \simeq 3$ mK, the corresponding temperature of the EN state splitting, the high-temperature approximation breaks down.

VI. CONCLUSIONS

A relaxation time the order of a millisecond for the nuclear ^{27}Al spin systems among themselves to a spin temperature T_s justifies the consideration of mutual flip-flop interactions during the time of the measurment (~ 18 h). Thus the proper theoretical local field average to be considered is $\frac{3}{2}3.4 = 5.1$ G. Since the experimental value is $\Delta h = 4.5 \pm 1.5$ G, it seems that the neglect of Fe^{3+}-Fe^{3+} contributions to the local field, as described in Sec. IV, is justified. (An Fe^{3+} contribution would worsen the agreement with theory.) The ME experimental spectrum of Fig. 3 then shows unambiguously the effect of nuclear dipole broadening.

We would like to comment upon the connection between our measurements and previous ME work in which nuclear dipole broadening was important. To detect nuclear dipole effects in paramagnetic Fe^{3+} ME spectra it is necessary to observe spectra from the $|\pm\frac{1}{2}\rangle$ doublet which is sensitive to small (~ 5 G) magnetic fields. This must be done at approximately zero applied field and presumably at low temperatures.

Benefiting from a large CF interaction ($D \simeq 10$ cm^{-1}), Lang *et al.*[15] have observed isolated spectra of the $|\pm\frac{1}{2}\rangle$ doublet at 4.2 K in acid met myoglobin. They pointed out the necessity of considering neighboring nuclear dipoles in analyzing the spectra. Using a random field model with unspecified nuclear dipole interaction, Vicarro *et al.*[16] calculated theoretical spectra which approximated the experimental results of Lang *et al.*[15] Shenoy and Dunlap[17] improved the calculation, to achieve a good fit, by incorporating relaxation effects as well as nuclear dipole fields.

It seems to us that our measurements deal with a simpler situation in that relaxation effects are absent, the form of the nuclear dipole field is known and a single crystal is used.

ACKNOWLEDGMENT

We wish to thank Dr. G. K. Wertheim for providing us with the $Al_2O_3(Fe^{3+})$ crystals and also for his interest in this work.

*Present address: Department of Physics, The John Hopkins University, Baltimore, Md. 21218.

[1]H. H. Wickman and G. K. Wertheim, Phys. Rev. 148, 211 (1966).

[2]C. E Johnson, T. E. Cranshaw, and M. S. Ridout, in *Proceedings of the International Conference on Magnetism, Nottingham, 1964* (The Institute of Physics and the Physical Society, London, 1964), pp. 459–461.

[3]G. K. Wertheim and J. P. Remeika, in *Proceedings of the XIII Colloque Ampere, Louvain, Belgium, 1964* (North-Holland, Amsterdam, 1965), pp. 147–161.

[4]J. Hess, A. Levy, and U. Schmid, Cryogenics 17, 501 (1977).

[5]A. M. Afanas'ev and Yu. M. Kagan, Zh. Eksp. Teor. Fiz. Pis'ma Red. 8, 620 (1968) [JETP Lett. 8, 382 (1968)].

[6]A. Abragam and B. Bleaney, *Electron Paramagnetic Resonance of Transition Ions* (Oxford, Oxford, 1970), Sec. 15.8.

[7]A. Levy, Ph.D. thesis (The Hebrew Univeristy of

Jerusalem, 1979) (unpublished).
[8]G. K. Wertheim and J. P. Remeika, Phys. Lett. 10, 14 (1964).
[9]C. M. Lederer, J. M. Hollander, and I. Perlman, *Table of Isotopes* (Wiley, New York, 1967).
[10]A. Abragam, *The Principles of Nuclear Magnetism* (Oxford, Oxford, 1961), Chap. IV, Eq. (39).
[11]H. B. Callen and T. A. Walton, Phys. Rev. 83, 34 (1951).
[12]The formulation and notation used here follows the treatment of L. D. Landau and E. M. Lifshitz, *Statistical Physics* (Pergamon, New York, 1970), Sec. 126.
[13]H. M. Rosenberg, *Low Temperature Solid State Physics* (Oxford, Oxford, 1963), Sec. 3.12.
[14]R. Berman, E. L. Foster, and J. M. Ziman, Proc. R. Soc. London Ser. A 231, 130 (1955).
[15]G. Lang, T. Asakura, and T. Yonetani, Phys. Rev. Lett. 24, 981 (1970).
[16]P. J. Viccaro, F. de S. Barros, and W. T. Oosterhuis, Phys. Rev. B 5, 4257 (1972).
[17]G. K. Shenoy and B. D. Dunlap, Phys. Rev. B 13, 1353 (1976).